

**Alpha-band oscillations track the retrieval of precise spatial representations from  
long-term memory**

David W. Sutterer<sup>1,2\*</sup>, Joshua J. Foster<sup>1,2</sup>, John T. Serences<sup>3,4</sup>,  
Edward K. Vogel<sup>1,2</sup>, and Edward Awh<sup>1,2\*</sup>

<sup>1</sup>Department of Psychology, University of Chicago

<sup>2</sup>Institute for Mind and Biology, University of Chicago

<sup>3</sup>Department of Psychology, University of California, San Diego

<sup>4</sup>Neuroscience Graduate Program, University of California, San Diego

**Running Title:** Alpha-band oscillations track spatial memory retrieval

\*Corresponding Authors:

David Sutterer  
david.w.sutterer@vanderbilt.edu  
Department of Psychology  
111 21<sup>st</sup> St  
Nashville, TN, 37212

or

Edward Awh  
awh@uchicago.edu  
Institute for Mind and Biology  
940 E 57<sup>th</sup> St  
Chicago, IL 60637

## 1 **Abstract**

2           A hallmark of episodic memory is the phenomenon of mentally re-experiencing the  
3 details of past events, and a well-established concept is that the neuronal activity that mediates  
4 encoding is reinstated at retrieval. Evidence for reinstatement has come from multiple modalities,  
5 including functional Magnetic Resonance Imaging (fMRI) and electroencephalography (EEG).  
6 These EEG studies have shed light on the time-course of reinstatement, but have been limited to  
7 distinguishing between a few categories. The goal of this work was to use recently developed  
8 experimental and technical approaches, namely continuous report tasks and inverted encoding  
9 models (IEMs), to determine which frequencies of oscillatory brain activity support the retrieval  
10 of precise spatial memories. In Experiment 1, we establish that an inverted encoding model  
11 applied to multivariate alpha topography tracks the retrieval of precise spatial memories. In  
12 Experiment 2, we demonstrate that the frequencies and patterns of multivariate activity at study  
13 are similar to the frequencies and patterns observed during retrieval. These findings highlight the  
14 broad potential for using encoding models to characterize long-term memory retrieval.

15 **New and noteworthy:**

16           Previous EEG work has shown that category-level information observed during encoding  
17 is recapitulated during memory retrieval, but studies with this time-resolved method have not  
18 demonstrated the reinstatement of feature-specific patterns of neural activity during retrieval.  
19 Here we show that EEG alpha-band activity tracks the retrieval of spatial representations from  
20 long-term memory. Moreover, we find considerable overlap between the frequencies and  
21 patterns of activity that track spatial memories during initial study and at retrieval.

22 **Keywords**

23 alpha, EEG, inverted encoding model, memory precision, spatial memory

## 24 Introduction

25 The retrieval of episodic memories is defined by the phenomenon of re-experiencing the  
26 details of past events, and is supported by *reinstatement*, the reactivation of neural activity that  
27 was present at encoding. Considerable support for this view has come from functional magnetic  
28 resonance imaging (fMRI) studies, which have shown that sensory regions involved in the initial  
29 processing of information are re-engaged at retrieval (Wheeler et al., 2000; Wagner et al., 2005;  
30 Danker and Anderson, 2010). Furthermore, voxel-wise patterns of activity within these regions  
31 during memory retrieval resemble activity seen during encoding (Polyn et al., 2005; Ritchey et  
32 al., 2013; Bosch et al., 2014; Hindy et al., 2016). Recent work has shown that reinstatement is  
33 evident in more time-resolved measures of neural activity, such as electroencephalography  
34 (EEG) and magnetoencephalography (MEG), providing an important complement to fMRI  
35 decoding because it reveals the temporal dynamics of retrieval. However, although EEG enables  
36 temporally resolved tracking of retrieved information, it has been limited to decoding coarse  
37 information, such as the category of a retrieved paired associated or the task performed at  
38 encoding (Wimber et al., 2012; Morton et al., 2013; Jafarpour et al., 2014; Johnson et al., 2015;  
39 Waldhauser et al., 2016). Thus, it remains to be seen whether EEG activity enables temporally  
40 resolved tracking of the retrieval of precise visual feature values that are associated with specific  
41 items.

42 Here, we measured EEG activity during the encoding and recall of precise spatial  
43 locations from long-term memory (LTM) and applied an inverted encoding model (IEM) to the  
44 topography of oscillatory activity on the scalp. IEMs have provided a useful approach for  
45 reconstructing precise spatial representations from fMRI and EEG activity (Sprague and  
46 Serences, 2013; Sprague et al., 2014, 2016, Foster et al., 2016, 2017b). Thus, we expected that

47 IEMs might also prove an effective tool for tracking the retrieval of precise spatial memories.  
48 Critically, this approach also allowed us to test another open question: What frequency bands  
49 carry spatial information retrieved from LTM?

50 On the one hand, theories about the role of rhythmic oscillations in memory have  
51 proposed that the same frequencies of oscillations coordinate specific cognitive operations at  
52 encoding and retrieval (Siegel et al., 2012; Watrous and Ekstrom, 2014; Watrous et al., 2015).  
53 Previous work using an IEM applied to alpha-band EEG activity, has successfully tracked covert  
54 spatial attention (Foster et al., 2017b), and spatial representations maintained in working memory  
55 (Sutterer et al., in press; Foster et al., 2016, 2017a), which leads to the prediction that alpha-band  
56 activity should also represent spatial locations retrieved from LTM. In line with this view, alpha-  
57 band activity has been shown to track hemifield-specific memory-guided attention (Stokes et al.,  
58 2012) and memory retrieval (Waldhauser et al., 2016), and the magnitude of alpha  
59 desynchronization tracks the number of items recalled from LTM (Fukuda and Woodman, 2017).

60 On the other hand, other frequency bands, especially theta and beta, are known to play  
61 important roles in long-term memory encoding and retrieval (Nyhus and Curran, 2010; Morton et  
62 al., 2013; Hsieh and Ranganath, 2014; Morton and Polyn, 2017; Kerren et al., 2018) and spatial  
63 navigation (Watrous et al., 2011; Bohbot et al., 2017). Moreover, recent fMRI studies have  
64 provided evidence that the constellations of cortical regions engaged (Xiao et al., 2017) and the  
65 strength of memory representations across regions (Favila et al., 2018) are not identical during  
66 encoding and memory retrieval raising the possibility that the frequency of oscillations  
67 representing information during encoding and retrieval might also vary. Thus, we investigated  
68 which frequency bands carry spatial information retrieved from LTM.

69 In two experiments, participants learned to associate objects with specific angular  
70 locations. Then, they were asked to precisely report the associated location when presented with  
71 an object cue. The IEM analysis revealed that oscillatory activity tracked the precise spatial  
72 position that was retrieved from LTM. Consistent with oscillatory reinstatement accounts, we  
73 found that spatially specific patterns of activity were largely restricted to the alpha band, the  
74 same frequency band that represents spatial locations held in WM (Sutterer et al., in press; Foster  
75 et al., 2016). Moreover, the alpha-band patterns observed during retrieval matched those  
76 observed during the initial encoding of the objects, in line with the hypothesis that encoding-  
77 related activity was reinstated during retrieval from LTM. Finally, the selectivity of alpha-band  
78 activity tracked memory performance as learning progressed from the first to second half of the  
79 session as well as the latency with which participants reported the target locations. Together  
80 these findings suggest that LTM retrieval elicits reinstatement of the spatially specific oscillatory  
81 activity that is observed during encoding, and that multivariate analysis of alpha-band activity  
82 provides a powerful measure of the timing and success of this basic cognitive process.

### 83 **Materials and Methods**

84 **Participants.** Sixty-nine adults (33 in Experiment 1, and 36 in Experiment 2; 18–35  
85 years old, 38 female) participated in the study for monetary compensation (\$10 per hour in  
86 Experiment 1, and \$15 per hour in Experiment 2). All participants reported normal or corrected-  
87 to-normal vision and provided informed consent according to procedures approved by the  
88 University of Oregon Institutional Review Board (Experiment 1) and the University of Chicago  
89 Institutional Review Board (Experiment 2).

90 **Participant exclusions for Experiment 1.** For Experiment 1, participants were excluded  
91 for poor performance on the task and excessive EEG artifacts. One participant did not return for

92 the second day of the experiment. One participant was excluded for poor performance on the first  
93 day (86.1° average response error across all day 1 tests) and data collection was terminated for  
94 one participant during the session for excessive artifacts. In addition, participants were excluded  
95 from further analysis if they had insufficient artifact-free trials (<550 trials). Artifact number  
96 exclusion criteria were set during data collection, but before the data were analyzed. Three  
97 participants were excluded due to excessive EEG artifacts. In the final sample, there were 27  
98 participants in Experiment 1 (mean number of artifact-free trials = 799, *SD* = 85).

99 **Participant exclusions for Experiment 2.** For Experiment 2, our target final sample size  
100 was 24 subjects. Participants were replaced for poor task performance or if too many trials were  
101 lost due to recording or ocular artifacts. One participant was excluded for poor performance on  
102 LTM trials (87.1° average response error across all retrieval tests), and data collection was  
103 terminated for three participants during the session for excessive artifacts. In addition,  
104 participants were excluded from further analysis if they had insufficient artifact-free trials (<450  
105 trials for encoding or retrieval). Artifact number exclusion criteria were set during data  
106 collection, but before the data were analyzed. We relaxed the exclusion criterion in Experiment  
107 2 because we obtained fewer trials per condition. Eight participants were excluded due to  
108 excessive EEG artifacts. In the final sample there were 24 participants in Experiment 2 (mean  
109 number of artifact-free encoding trials = 535, *SD* = 46 and recall trials = 545, *SD* = 39).

110 [Insert Figure 1 here]

111 **Apparatus.** Stimuli were presented in MATLAB using Psychtoolbox (Brainard, 1997;  
112 Pelli, 1997) and were presented on a 17-in. CRT monitor (60 Hz) for Experiment 1 and on a 24-  
113 in. LCD monitor (120 Hz) for Experiment 2.

114           **Experiment 1 task procedure.** The experiment was comprised of two sessions run on  
115 consecutive days (Figure 1a). On Day 1, participants were instructed to learn 120 object-location  
116 associations (see Figure 1a for example clip art) as accurately as possible for the test the next  
117 day. On Day 2, participants were cued with the object and asked to recall and report the  
118 associated location while we recorded EEG data.

119           On Day 1, all 120 object-location pairings were studied over three repetitions with  
120 interleaved retrieval practice. Each of these repetitions were randomly divided into 12 “mini-  
121 blocks”, in which 10 objects were presented followed by a final test on all objects in a random  
122 order. Specifically, 10 objects were serially presented in their respective spatial locations (1000  
123 ms per object, each object initiated by pressing spacebar). Next, each of the 10 objects were  
124 presented at fixation in a random order (1000 ms per object), and participants clicked that  
125 object’s location along a ring (unspeeded). Recall performance was assessed by calculating the  
126 response error (i.e., difference between the presented and reported location, ranging between –  
127 180° and 180°). After each response, participants were presented with the object in its correct  
128 location and the response error (500 ms). After completing these mini-blocks, participants again  
129 retrieved all 120 objects in a random order. One participant did not complete the final retrieval  
130 on the third run, and one participant accidentally aborted the experiment during the presentation  
131 of the first 10 objects before completing the rest of the session.

132           On Day 2, participants repeatedly retrieved the location of all 120 objects while we recorded  
133 EEG activity (Figure 1a). During each repetition (7–8 in total), the objects were presented in a  
134 random order. Each retrieval trial was initiated by a space press. After a variable interval of 1100  
135 to 1500ms, an object was presented at fixation along with the response ring. Participants were  
136 instructed to maintain fixation and to avoid blinking or moving the mouse from trial initiation



137 until the cursor appeared 1250ms after the onset of the memory cue. Participants were also  
138 instructed to recall the location during the retrieval delay (1250 ms). After each response,  
139 participants were shown the correct location of the item along with a number denoting the  
140 magnitude of the error.

141 **Experiment 2 task procedure.** Experiment 2 was designed to examine encoding-  
142 retrieval similarity within a single session. As such, the experiment was modified to take place  
143 within one day by reducing the total number of objects (80 vs. 120). Participants were instructed  
144 to learn object-location associations as accurately as possible and that they would alternate  
145 between studying and being tested on these associations (Figure 1c).

146 During the study session, participants studied and then recalled each item during each  
147 trial. Each study trial was initiated by a space press. After a variable interval of 500 to 800 ms, an  
148 object was centrally presented (Figure 1c) along with a dot at the paired location (500 ms  
149 stimuli) followed by a blank delay (1250 ms). To prevent participants from using a part of the  
150 object as a reference to remember the associated location, we randomly varied the orientation of  
151 each object ( $-45$  to  $45^\circ$ ) for each presentation. As in Experiment 1, participants then reported the  
152 to-be-remembered location by clicking on the response ring (unspedded). Participants were  
153 instructed to click with the left mouse button if they were confident in their response, and to click  
154 with the right mouse button if they felt that they were guessing. Both confident and guess  
155 responses were used for subsequent analyses. After each response, participants were shown the  
156 correct location of the item along with a number denoting the magnitude of the error. After  
157 studying all 80 objects, participants underwent another retrieval test for all objects in a random  
158 order (Figure 1c). The only difference between study and recall trials was the presence of the  
159 peripheral dot.

160           **Stimuli.** In Experiment 1, 120 clip art objects (e.g., animals, plants, objects) were  
161 selected from the Sutterer and Awh (2016) clip art library. All objects were randomly assigned to  
162 unique angular locations (0–360°, 3° steps) for each participant. On Day 1, the viewing distance  
163 was ~80 cm (1.9° stimuli, 5° response ring, 0.3° fixation dot). On Day 2, the viewing distance  
164 was ~100cm (1.5° stimuli, 4° response ring, 0.25° fixation dot). The background of the screen  
165 was medium gray, all objects appeared in the color cyan, the response ring was dark grey, and  
166 the fixation dot was rendered in black.

167           In Experiment 2, 80 of the objects from Experiment 1 were randomly paired with a  
168 unique location drawn from all 360° of possible locations. In order to assure that the entire space  
169 was used, assignment of locations was constrained such that an equal number of locations were  
170 drawn without replacement from eight bins each spanning 45 degrees of the possible space. The  
171 viewing distance was ~100 cm (1.2° stimuli, 4° response ring, 0.25° fixation dot). The  
172 background of the screen was again medium gray, all objects appeared in the color cyan, and the  
173 response ring and the fixation dot were dark grey.

174           **Modeling of Response Errors.** Response error was measured as the number of degrees  
175 between the presented angular location and the reported angular location. Errors ranged from 0°  
176 (a perfect response) to  $\pm 180^\circ$  (a maximally imprecise response). For each run (Figure 1b), we  
177 calculated the average absolute response error for the artifact free trials. Error distributions of  
178 this sort have been shown to be well described by a mixture of a uniform distribution for guesses  
179 and a Von Mises distribution for correct responses (Zhang and Luck, 2008; Brady et al., 2013).  
180 We used MemToolbox (Suchow et al., 2013) to calculate the probability of retrieval ( $P_{mem}$ ),  
181 precision ( $SD$ ), and the bias ( $\mu$ ) of each participants responses.

182           **EEG acquisition.** In Experiment 1, EEG was recorded with 20 tin electrodes mounted in  
183 an elastic cap (Electro-Cap International, Eaton, OH). We recorded from International 10/20  
184 sites F3, FZ, F4, T3, C3, CZ, C4, T4, P3, PZ, P4, T5, T6, O1, and O2, along with five  
185 nonstandard sites (OL, OR, PO3, PO4, POz). All sites were recorded with a left-mastoid  
186 reference, and were re-referenced offline to the algebraic average of the left and right mastoids.  
187 To detect horizontal eye movements, electrodes were placed ~1 cm from the canthi of each eye  
188 to record horizontal electrooculogram (EOG). To detect blinks and vertical eye movements, a  
189 single electrode was placed under the center of the right eye and referenced to the left mastoid to  
190 record vertical EOG. The EEG and EOG data were amplified with an SA Instrumentation  
191 amplifier, filtered (0.01–80 Hz), and digitized (250 Hz) using LabVIEW 6.1 running on a PC.

192           In Experiment 2, EEG was recorded from 30 active Ag/AgCl electrodes (Brain Products  
193 actiCHamp, Munich, Germany) mounted in an elastic cap positioned according to the  
194 International 10-20 system Fp1, Fp2, F7, F3, F4, F8, Fz, FC5, FC6, FC1, FC2, C3, C4, Cz, CP5,  
195 CP6, CP1, CP2, P7, P8, P3, P4, Pz, PO7, PO8, PO3, PO4, O1, O2, Oz. A ground electrode was  
196 placed in the elastic cap at position FPz. Data were referenced online to the right mastoid and re-  
197 referenced offline to the algebraic average of the left and right mastoids. Incoming data were  
198 filtered (0.01– 80 Hz) and recorded with a 500 Hz sampling rate using Brain Vision Recorder  
199 running on a PC. To detect eye movements and blinks, we used eye tracking to monitor gaze  
200 position and electrooculogram (EOG) activity recorded with five electrodes (~1cm from the  
201 outer canthi of each eye, above/below the right eye, and a ground electrode placed on the left  
202 cheek).

203           **Artifact Rejection.** Data from both experiments were visually inspected for EOG and  
204 EEG artifacts. Trials containing blinks, eye movements, blocking, and muscle artifacts were

205 excluded from analysis. One electrode for one participant in Experiment 2 was also rejected  
206 during recording because it had malfunctioned. We also monitored gaze position during  
207 Experiment 2 using a desk-mounted infrared eye tracking system (EyeLink 1000 Plus, SR  
208 Research, Ontario, Canada). Gaze position data for Experiment 2 were also visually inspected for  
209 ocular artifacts. For the analysis of gaze position, we further excluded trials in which the eye  
210 tracker was unable to detect the pupil, operationalized as any trial in which the horizontal gaze  
211 position was more than  $15^\circ$  from fixation or the vertical gaze position was more than  $8.5^\circ$  from  
212 fixation. We collected useable gaze position data (500 Hz sampling rate) for 18 of 24  
213 participants.

214       Removal of trials with ocular artifacts was effective: maximum variation in grand-  
215 averaged HEOG waveforms by remembered location bin was  $< 2.5 \mu\text{V}$  for Experiment 1 and  $< 2$   
216  $\mu\text{V}$  for both the encoding and retrieval in Experiment 2. Thus, eye movements in both  
217 experiments corresponded to variations in eye position of  $< 0.2^\circ$  of visual angle (Lins et al.,  
218 1993), roughly the size of the fixation dot. Analysis of the subset of participants (18) for whom  
219 we were able to obtain reliable gaze position data in Experiment 2 corroborates the HEOG data  
220 obtained from all participants. Variation in grand-average horizontal gaze position as a function  
221 of remembered location was  $< 0.11^\circ$  for encoding and  $< 0.08^\circ$  of visual angle for retrieval.  
222 Variation in grand-average vertical gaze position data by remembered location was  $< 0.14^\circ$  for  
223 encoding and  $< 0.09^\circ$  of visual angle for retrieval. For comparison, HEOG for these participants  
224 showed a  $< 2.1 \mu\text{V}$  maximum variation which also corresponds to  $< 0.2^\circ$  of visual angle.

225       **Time-frequency analysis.** To calculate frequency specific activity at each electrode we  
226 first band-pass filtered the raw EEG data using EEGLAB (eegfilt, see Delorme and Makeig,  
227 2004). Alpha band analyses were band-pass filtered between 8 to 12 Hz, which is consistent with

228 our prior work (Foster et al., 2016). For our exploratory analysis of the full range of frequencies,  
 229 we band-pass filtered the data at 1 Hz intervals (4–50 Hz, down-sampled to 20 Hz,

230 
$$\text{filter order: } 3 \times \frac{\text{sampling rate}}{\text{low-pass cutoff}}$$

231 We then applied a Hilbert transform (MATLAB Signal Processing Toolbox) and squared the  
 232 complex magnitude of the complex analytic signal for each trial to calculate instantaneous power  
 233 before averaging across trials.

234 **Inverted encoding model.** Following our prior work (Sutterer et al., in press; Foster et  
 235 al., 2016), we estimated spatially selective channel-tuning functions (CTFs) from the  
 236 multivariate topographic distribution of oscillatory power across electrodes. We assumed that the  
 237 power at each electrode reflects the weighted sum of eight spatially selective channels, which we  
 238 assume reflect the response of neural populations. Each spatially selective channel was tuned for  
 239 a different angular location (Brouwer and Heeger, 2009; Sprague and Serences, 2013; Sprague et  
 240 al., 2015; Foster et al., 2016). We modeled the response profile of each spatial channel across  
 241 angular locations as a half sinusoid raised to the seventh power:

242 
$$R = \sin(0.5\theta)^7,$$

243 where  $\theta$  is angular location (0–359°), and  $R$  is the response of the spatial channel in arbitrary  
 244 units. This response profile was circularly shifted for each channel such that the peak response of  
 245 each spatial channel was centered over one of the eight location bins which were created relative  
 246 to the original position of the stimulus. These 8 location bins each spanned 45° and were  
 247 centered on 22.5°, 67.5°, 112.5° etc. for Experiment 1 and on 0°, 45°, 90° etc. for Experiment 2.  
 248 Bin centers for each experiment were chosen prior to data collection.

249 An IEM routine was applied to each time point in the alpha-band analyses and to each  
 250 time-frequency point in the time-frequency analyses. We partitioned our data into independent

251 sets of training data and test data (for details see the Assigning trials to training and test sets  
 252 section). This routine proceeded in two stages (train and test). In the training stage, training data  
 253  $B_1$  were used to estimate weights that approximate the relative contribution of the eight spatial  
 254 channels to the observed response measured at each electrode. Let  $B_1$  ( $m$  electrodes  $\times$   $n_1$   
 255 observations) be the power at each electrode for each measurement in the training set,  $C_1$  ( $k$   
 256 channels  $\times$   $n_1$  measurements) be the predicted response of each spatial channel (determined by  
 257 the basis functions) for each measurement, and  $W$  ( $m$  electrodes  $\times$   $k$  channels) be a weight matrix  
 258 that characterizes a linear mapping from “channel space” to “electrode space”. The relationship  
 259 between  $B_1$ ,  $C_1$ , and  $W$  can be described by a general linear model of the form:

$$B_1 = WC_1$$

260 The weight matrix was obtained via least-squares estimation as follows:

$$\widehat{W} = B_1 C_1^T (C_1 C_1^T)^{-1}$$

261 In the test stage we inverted the model to transform the observed test data  $B_2$  ( $m$  electrodes  $\times$   $n_2$   
 262 observations) into estimated channel responses,  $C_2$  ( $k$  channels  $\times$   $n_2$  measurements), using the  
 263 estimated weight matrix,  $\widehat{W}$ , that we obtained in the training phase:

$$\widehat{C}_2 = (\widehat{W}^T \widehat{W})^{-1} \widehat{W}^T B_2$$

264 Each estimated channel response function was then circularly shifted to a common center (i.e.,  $0^\circ$   
 265 on the “Channel Offset” axis of Figure 2a) by aligning the estimated channel responses to the  
 266 channel tuned for the cued/target location to yield the CTF averaged across the eight  
 267 remembered locations.

268 Finally, because the exact contributions of each spatial channel to each electrode (i.e., the  
 269 channel weights,  $W$ ) varies across participants, we applied the IEM routine separately for each  
 270 participant, and statistical analyses were performed on the reconstructed CTFs. This approach

271 allowed us to disregard differences in how location-selective activity is mapped to scalp-  
272 distributed patterns of power across participants, and instead focus on the profile of activity in  
273 the common stimulus or “information” space (Sprague et al., 2015; Foster et al., 2016).

274 **Assignment of trials to training and test sets.** Artifact free trials were partitioned  
275 equally into three independent sets to be used as training and test data for the IEM procedure (see  
276 Inverted Encoding Model). We down-sampled the data so that each set contained an equal  
277 number of trials, and that each location bin within a set also contained the same number of trials.  
278 For each of these sets we averaged power across trials for each location bin. We used a cross  
279 validation routine such that two sets of estimated power served as the training data and the  
280 remaining set served as the test data. We applied the IEM routine using each of the three  
281 matrices as test data, and the remaining two matrices as training data. The resulting CTFs were  
282 averaged across each test set.

283 For the analysis in which we ruled out the possibility that the IEM was detecting object-  
284 specific information, we assigned all trials with the same object to the same partition. After  
285 completing this additional step, we equated trials across sets and bins in the same manner  
286 described above.

287 For analyses in which we examined how within participant changes in selectivity related  
288 to behavior, we first down-sampled to equate the number of trials assigned from each location  
289 across conditions. After completing this additional step, we equated trials across sets and bins in  
290 the same manner described above. Finally, we employed the same training procedure described  
291 above (2/3 of the total data), but split the final test set into our comparisons of interest. Thus, we  
292 used the same training data for both conditions and only the test data varied for each comparison.

293 For analyses that assessed relationships between CTF selectivity and behavior across  
294 participants we down-sampled the number of trials assigned to each location bin for each of the  
295 three sets to be equal to the smallest number of trials assigned to each bin in each set for any  
296 participant. This down sampling approach precluded individual differences in CTF selectivity  
297 driven by the number of the trials included in the analysis for each participant.

298 In Experiment 2, we sought to compare encoding and retrieval related activity. We  
299 closely followed the procedure that examined retrieval-related activity alone, by training on 2/3  
300 of the encoding data and testing on 1/3 of the retrieval data. By maintaining these same ratios of  
301 training to test data, we could more directly compare the results from encoding and retrieval.

302 **Resampling random assignment.** To avoid spurious results due to the random  
303 assignment of trials, we repeated each analysis multiple times with a different random  
304 assignment of trials. When comparing between conditions, we conducted 500 iterations per time  
305 point. When comparing against a permuted null distribution (which is a time-consuming  
306 procedure), we conducted 10 iterations per time point, given the computational time needed for  
307 each analysis. In order to decrease computation time further for the 4–50 Hz time-frequency  
308 analysis, we down sampled the data matrix of power values to one sample every 20 ms. We  
309 down sampled after calculating power so that down sampling did not affect our calculation of  
310 power. The data matrix was not down-sampled for analyses restricted to the alpha band.

311 **Calculating CTF Selectivity.** To quantify selectivity at each time point we calculated the  
312 slope of the CTF via linear regression. We collapsed across channels of equidistance (e.g.,  $\pm 2$   
313 bins). As such, higher slope values indicate greater CTF selectivity while lower values indicate  
314 less CTF selectivity.



315 To test whether CTF selectivity was reliably above chance, we tested whether CTF slope  
316 was greater than zero using a one-sample  $t$  test. Because mean CTF slope may not be normally  
317 distributed under the null hypothesis, we employed a Monte Carlo randomization procedure to  
318 empirically approximate the null distribution of the  $t$  statistic. To generate our null distribution,  
319 we randomly shuffled the remembered location labels in each training/test set so that the labels  
320 were random with respect to the observed responses at each electrode. We then repeated 1000  
321 iterations of this randomization procedure to obtain a null distribution of  $t$  statistics at each time  
322 point.

323 Finally, to test whether CTF selectivity was reliably above chance we employed a  
324 nonparametric cluster approach that corrects for multiple comparisons by taking into account  
325 auto-correlation in time and frequency (Maris and Oostenveld, 2007; Cohen, 2014). Specifically,  
326 we applied a  $t$ -value threshold corresponding to  $p < .05$  (Experiment 1:  $t = 1.706$ ; Experiment 2:  
327  $t = 1.714$ ) to identify clusters of pixels (time and frequency analysis) or adjacent time points  
328 (alpha only analysis). At the same time, we applied the same threshold to each permutation and  
329 calculated the largest summed- $t$  statistic for any cluster in the permutation, resulting in a  
330 distribution of maximal summed  $t$ -statistics for our permuted null distribution. Finally, the sizes  
331 of the significant clusters of the non-permuted data were thresholded such that only clusters  
332 larger than the 95<sup>th</sup> percentile of the permuted distribution were considered reliable (Type 1 error  
333 less than .05). Therefore, our cluster test was a one-tailed test, corrected for multiple  
334 comparisons.

## 335 Results

### 336 Experiment 1

337 Experiment 1 was designed to test whether EEG activity tracked the retrieval of precise  
338 spatial locations from LTM. The design includes two important properties. First, we asked  
339 subjects to precisely report a remembered location using a continuous report procedure (Wilken  
340 and Ma, 2004; Zhang and Luck, 2008). This provides a sensitive test of memory accuracy as the  
341 deviation from the correct location. Second, we recorded EEG activity during memory retrieval  
342 for the purposes of building and evaluating an encoding model. This inverted encoding model  
343 (IEM) can track memory retrieval as a graded function of spatial location.

344 **Behavioral performance.** On Day 1, participants studied 120 object-location  
345 associations (Figure 1a). On Day 2, participants returned for a retrieval session in which we  
346 recorded EEG. Participants received feedback based on their response error ( $-180^\circ$  to  $180^\circ$ ).  
347 During both days, their performance improved (Figure 1b). During Day 1, average response error  
348 improved significantly from the first ( $M = 53.6^\circ$ ,  $SD = 17.7^\circ$ ) to the final test ( $M = 17.6^\circ$ ,  $SD =$   
349  $11.1^\circ$ ) of the session ( $t(26) = 13.2$ ,  $p < .001$ , two-tailed). As a result on continued feedback,  
350 memory also improved from the first ( $M = 25.2^\circ$ ,  $SD = 14.1^\circ$ ) to the final test ( $M = 12.7^\circ$ ,  $SD =$   
351  $9.3^\circ$ ) during the second session ( $t(26) = 7.3$ ,  $p < .001$ , two-tailed).

352 **Alpha-band (8–12 Hz) topography tracks spatial representations retrieved from**  
353 **LTM.** In Experiment 1, we tested whether oscillatory EEG activity tracks the time-resolved  
354 retrieval of precise spatial memories. Because we have previously found that alpha-band activity  
355 tracks spatial locations held in working memory (Foster et al., 2016), we were *a priori* interested  
356 in whether alpha-band power would also track locations retrieved from long-term memory. Thus,  
357 we used an IEM to test whether the multivariate topography of alpha-band power tracked  
358 locations retrieved from long-term memory. If the pattern of alpha-band power contains spatially  
359 selective information about the remembered location, we would expect to see a channel tuning

360 function (CTF) with a peak response in the channel tuned for the remembered location (a  
361 channel offset of  $0^\circ$  in Figure 2) following the retrieval cue. This pattern can be quantified as  
362 slope across the position channels as distance from the retrieved location increases. A slope of  
363 zero reflects no spatial selectivity in the CTF, while a positive slope reflects spatial selectivity for  
364 the location associated with the cue. To test this hypothesis, we conducted a permutation test (see  
365 Materials and Methods) to determine at which time points we observed a CTF slope that was  
366 reliably above zero. We detected reliable selectivity for spatial information (i.e., slopes  $> 0$ ) that  
367 was sustained during the retrieval interval (588 – 1250ms; Figure 2a).

368 [Insert Figure 2 here]

369 One possibility is that this graded tuning is an artifact of our selection of a graded basis  
370 set (Saproo and Serences, 2014; Ester et al., 2015; Foster et al., 2016). To investigate this  
371 possibility, we reran this analysis using a delta-function basis set that predicts a peak response in  
372 the preferred channel and no response in adjacent channels. If the topography of alpha power  
373 represents spatial locations in a graded manner, we would still expect a graded pattern of  
374 responses. Instead, if the observed results were driven by our selection of a basis set, we would  
375 expect a peak response in the correct bin and a little to no response in all other bins. Using a  
376 delta function basis set, we observed a graded pattern of responses across remembered locations  
377 (Figure 2b) that is similar to the pattern of activity we see when we apply the standard basis set  
378 (Figure 2c). This suggests that our results are not an artifact of our selection of a basis set, but  
379 reflect a real graded tuning profile during the retrieval of spatial memories.

380 Although the aggregate results revealed that channel activity peaked at the remembered  
381 location and dropped in a graded fashion as the distance from that location increased, this  
382 analysis did not establish that this orderly pattern was present at each location. Indeed, a coarser

383 hemi-field or quadrant-based signal could produce such a pattern. If alpha-band activity precisely  
384 tracks retrieved spatial locations, we should observe a graded pattern for each remembered  
385 location. We examined the average channel response during time points where we previously  
386 observed reliable spatial selectivity (588–1250ms) for eight location bins separately. The channel  
387 response for each location revealed graded information throughout the same window, and the  
388 channel responses for all locations were significant (All slopes  $> 0.05$ , all  $p$ 's  $< .002$ ). Therefore,  
389 alpha-band CTFs track memory retrieval of a precise spatial location.

390 **Identifying frequencies that track the retrieval of spatial location.** A motivating  
391 question for the present work was whether spatially selective information was specific to alpha-  
392 band activity. On the one hand, prior work has found that alpha-band activity selectively tracks  
393 spatial locations that are covertly attended (Foster et al., 2017b) or held in working  
394 memory (Foster et al., 2016). On the other hand, theta-band (4–7 Hz) and beta-band (16–25 Hz)  
395 activity are known to play an important role in long-term memory (Nyhus and Curran, 2010;  
396 Morton and Polyn, 2017; Kerren et al., 2018). Therefore, we performed the same IEM analysis  
397 at each frequency and time point from 4–50 Hz to test whether other frequency bands also  
398 carried spatially selective information about the remembered location. We conducted a  
399 permutation test at each frequency and time point and used a cluster correction to identify  
400 frequencies with CTFs that were reliably above zero (Figure 3a). The most robust and sustained  
401 selectivity was in the alpha band (410ms – 1250ms).

402 [Insert Figure 3 here]

403 **Spatially selective alpha-band activity generalizes across visual objects associated**  
404 **with the same spatial location.** For each participant, each object was associated with a unique  
405 location such that object and position were confounded within this analysis. Thus, it is possible

406 that the selectivity we observed across some or all frequencies, reflects patterns of activity  
407 elicited by the cue rather than activity related to the retrieval of a spatial position. To investigate  
408 this, we re-ran the analysis while ensuring that distinct items were included in the training and  
409 test sets (see Materials and Methods). Despite this constraint, we observed similar results (Figure  
410 3b), confirming that the sustained spatial selectivity we observed reflected the position  
411 associated with each cue rather than the cue itself. Thus, for all subsequent IEM analyses we do  
412 not constrain assignment to training and test sets by cue. We also observed a brief period of  
413 spatial selectivity in the beta range (16–25 Hz); however, we note that this activity was not  
414 observed when we did not constrain the assignment of items to training and test sets.

415 **Spatial selectivity of alpha-band activity increases with repetition and feedback.** A  
416 consequence of providing feedback during Day 2 is that memory performance improved  
417 throughout the session. To examine whether alpha-band CTFs tracked these broad behavioral  
418 improvements, we split the test data into the first half and second half of trials. Behaviorally, we  
419 observed that memory performance improved from the first half ( $M = 20.3^\circ$ ,  $SD = 11.9^\circ$ ) to the  
420 second half ( $M = 13.9^\circ$ ,  $SD = 9.4^\circ$ ) of the session ( $t(26) = 7.2$ ,  $p < .001$ , two-tailed, Figure 4a).  
421 Furthermore, a mixture model was used to assess whether these decreases in average response  
422 error were driven by changes in the probability of retrieval and/or mnemonic precision (see  
423 Materials and Methods). During Day 2, the probability of retrieval ( $P_{mem}$ ) increased over time  
424 (first half:  $M = 86.3\%$ ,  $SD = 13.6\%$ ; second half:  $M = 93.6\%$ ,  $SD = 9.5\%$ ;  $t(26) = -6.3$ ,  $p$   
425  $< .001$ , two-tailed) and mnemonic precision improved over time (first half:  $M = 13.6^\circ$ ,  $SD = 3.7^\circ$ ;  
426 second half:  $M = 12.3^\circ$ ,  $SD = 4.1^\circ$ ,  $t(26) = 5.52$   $p < .001$ , two-tailed). If alpha-band CTFs are  
427 sensitive to memory performance, we would expect greater spatial selectivity in the second vs.  
428 first half of the session. To test this prediction, we isolated the time points where aggregate data

429 revealed significant alpha CTFs (Fig 2a; 588ms after cue onset until the response), and then  
430 compared average CTF slope across the first and second halves of the study. Indeed, spatial  
431 selectivity was significantly higher for the second half (CTF slope,  $M = 0.085$ ,  $SD = 0.061$ )  
432 relative to the first half ( $M = 0.06$ ,  $SD = 0.055$ ) of the experiment ( $t(26) = -3.29$ ,  $p = .003$ , two-  
433 tailed; Figure 4b).

434 [Insert Figure 4 here]

435 This reveals that alpha-band activity tracks the improvement in memory performance  
436 across learning episodes. Finally, CTF selectivity across the same window did not predict  
437 between-subject variations in the accuracy of recall ( $\rho(26) = -.11$ ,  $p = .6$ ). This null result could  
438 have numerous explanations but here we offer one hypothesis. While we instructed participants  
439 to immediately recall the location that corresponded to the object cue, it may be that some  
440 participants waited longer than others to call the correct location to mind while other participants  
441 relied on a more prospective strategy in which they immediately recalled the target location. This  
442 kind of strategic difference could yield large differences in mean CTF slope that may have been  
443 unrelated to whether the critical item could be retrieved. Indeed, the response time analysis in the  
444 next section lends further plausibility to this hypothesis.

445 **Spatially selective alpha-band activity tracks within- and between-subject variations**  
446 **in response latency.** The latency of memory retrieval varied across trials and participants to a  
447 large extent (see Fig 5a). To examine whether alpha-band CTFs tracked these behavioral  
448 differences in response time (RT), we split the test data into two halves based on the median RT  
449 (average fast RT:  $M = 854\text{ms}$ ,  $SD = 240\text{ms}$ ; average slow RT:  $M = 1961\text{ms}$ ,  $SD = 1055\text{ms}$ ). If  
450 alpha-band CTFs track the latency of memory retrieval, we would expect greater location  
451 selectivity on trials in which participants responded more quickly. Indeed, location selectivity

452 was significantly greater when participants responded more quickly ( $M = 0.085$ ,  $SD = 0.054$ )  
453 than when they responded slowly ( $M = 0.051$ ,  $SD = 0.060$ ;  $t(26) = -4.29$ ,  $p < .001$ , two-tailed;  
454 Figure 5b). This pattern supports the hypothesis that participants responded more quickly when  
455 they had already retrieved the spatial information prior to the onset of the response cue, yielding  
456 a higher level of CTF selectivity during trials with faster responses.

457 [Insert Figure 5 here]

458 Across participants, we observed substantial variation in median RTs (range = 504 –  
459 2025 ms). To examine whether alpha-band CTFs tracked these individual differences in  
460 behavior, we tested whether there was a correlation between median RT and the selectivity of  
461 alpha-band CTFs (measured as slope). We predicted that participants who responded more  
462 quickly (i.e., faster RTs) would also have greater spatial selectivity (i.e., higher CTF slope). We  
463 observed a trending negative relationship between RT and CTF slope, as predicted ( $\rho = -.36$ ;  $p =$   
464  $.07$ ; Figure 5c). In addition to reflecting differences in the immediate accessibility of spatial  
465 memories, this relationship could also be driven by individual differences in the extent to which  
466 participants engaged in prospective retrieval during the delay interval. This is our working  
467 hypothesis, given that the differences in response latency seemed too large to reflect differences  
468 in the immediate accessibility of the spatial memories alone.

## 469 **Experiment 2**

470 In Experiment 2, we replicated and extended Experiment 1 in two important ways. First,  
471 to further examine the relationship between alpha-band selectivity and memory performance, we  
472 recorded EEG data throughout the learning process, including the first retrieval attempts.  
473 Second, we recorded EEG during both encoding and retrieval, which allowed us to test the extent  
474 that retrieval-related oscillatory activity resembled encoding-related oscillatory activity.

475           **Behavioral performance.** During a single session, participants learned 80 object-  
476 location associations (Figure 1c) with interleaved study and retrieval. During study trials,  
477 participants actively maintained the associated spatial location over a 1250 ms delay interval.  
478 During retrieval trials, participants had to retrieve the associated spatial location from long-term  
479 memory. During study trials, memory performance was very accurate and improved modestly  
480 but reliably from the first half ( $M = 4.7^\circ$ ,  $SD = 1^\circ$ ) to the second half ( $M = 4.4^\circ$ ,  $SD = .9^\circ$ ) of the  
481 session ( $t(23) = 2.42$ ,  $p = .024$ , two-tailed; Figure 1d). Mixture modelling revealed that this  
482 change was due to an improvement in mnemonic precision (first half:  $M = 5.8^\circ$ ,  $SD = 1.2^\circ$ ;  
483 second half:  $M = 5.4^\circ$ ,  $SD = 1.1^\circ$ ;  $t(23) = 2.28$ ,  $p = .032$  two-tailed) while no change was  
484 observed for probability of retrieval (first half:  $M = 99.9\%$ ,  $SD = .29\%$ ; second half:  $M = 99.9\%$ ,  
485  $SD = .16\%$ ;  $t(23) = -.81$ ,  $p = .42$ , two-tailed), which was at ceiling. For the LTM retrieval trials,  
486 we observed a substantial improvement in memory performance across the session as learning  
487 progressed. Memory error decreased from the first half ( $M = 40.8^\circ$ ,  $SD = 14.0^\circ$ ) to the second  
488 half ( $M = 16.2^\circ$ ,  $SD = 11.9^\circ$ ;  $t(23) = 17.0$ ,  $p < .001$ , two-tailed; Figure 6a) of the experiment. We  
489 replicated our finding from Experiment 1 that the reduction in memory error was driven by both  
490 an increase in the probability of retrieval (first half:  $M = 61.1\%$ ,  $SD = 16.1\%$ ; second half:  $M =$   
491  $89.9\%$ ,  $SD = 13.9\%$ ;  $t(23) = -15.4$ ,  $p < .001$ , two-tailed) and an improvement in mnemonic  
492 precision (first half:  $M = 13.7^\circ$ ,  $SD = 4.4^\circ$ ; second half:  $M = 11.3^\circ$ ,  $SD = 2.7^\circ$ ;  $t(23) = 4.12$ ,  $p$   
493  $< .001$ , two-tailed). Thus, long-term memory improved throughout the session as participants  
494 learned the object-location associations.

495           One goal for Experiment 2 was to create a larger range of performance throughout the  
496 session in which EEG data were recorded. In line with this goal, we observed a much larger  
497 range in mean response error in Experiment 2 ( $71.0^\circ$  Run 1 –  $15.2^\circ$  Run 9; Figure 1d) than in



498 Day 2 of Experiment 1 (25.2° Run 1 – 12.3° Run 8), giving us the opportunity to apply the IEMs  
499 approach across the full trajectory of learning.

500 **Spatial selectivity of alpha-band activity increases with repetition and feedback.** In  
501 Experiment 1, alpha-band CTFs tracked retrieval of spatial locations from long-term memory.  
502 Furthermore, spatial selectivity of alpha-band CTFs increased as memory performance improved  
503 with repetition and feedback (Figure 4). Experiment 2 was designed to replicate and extend those  
504 results over a larger range of behavior. We predicted that alpha-band CTFs would demonstrate  
505 higher selectivity when memories were more accurate. In line with this prediction, the average  
506 selectivity (i.e., CTF slopes) was larger in the second half of the session ( $M = 0.048$ ,  $SD = 0.033$ )  
507 than in the first half ( $M = 0.012$ ,  $SD = 0.022$ ;  $t(23) = -4.79$ ,  $p < .001$ ; two-tailed; Figure 6b).  
508 Note, for this and all subsequent average CTF analyses, we averaged from 588 ms (the starting  
509 time point used in Experiment 1) until the onset of the response cue. Control analyses revealed  
510 that increases in alpha-selectivity across the session could not be attributed to increases in alpha  
511 power across the recoding session (Figure S1; <https://figshare.com/s/9f594406315b89b21e9a>).  
512 As in Experiment 1, CTF slope did not track memory performance between participants ( $\rho(23) =$   
513  $-.14$ ,  $p = .52$ ). Thus, the spatial selectivity of alpha activity tracked broad improvements in  
514 memory performance across the session, but not individual differences in memory performance.

515 [Insert Figure 6 here]

516 **Spatially selective alpha-band activity tracks response latency.** As in Experiment 1,  
517 we found that the selectivity of alpha-band CTFs tracked within- and between-subject variations  
518 in RT (Figure 7). A median split on RT revealed greater spatial selectivity for trials with fast RTs  
519 (CTF slope:  $M = 0.035$ ,  $SD = 0.03$ ) than trials with slow RTs ( $M = 0.021$ ,  $SD = 0.018$ ,  $t(23) = -$   
520  $2.53$ ,  $p = .018$ , two-tailed; Figure 7b). We also replicated our finding that participants with faster

521 RTs showed greater spatial selectivity of alpha-band CTFs ( $\rho = -.49$ ;  $p = .02$ ; Figure 7c). This  
522 link between CTF slope and RTs may reflect strategic differences between participants who  
523 prospectively recalled the associated location quickly following cue onset and those that waited  
524 until closer to the response window to bring that information to mind.

525 [Insert Figure 7 here]

526 **Comparing frequency specificity at encoding and retrieval.** In Experiment 1, we  
527 found that oscillatory activity in the alpha band (8–12 Hz) tracked retrieved locations following a  
528 memory cue. In Experiment 2, we replicated this finding, with cluster corrected permutation tests  
529 showing that primarily oscillations between 8 and 12 Hz (~500–1500ms; Figure 8a), and to a  
530 lesser extent, oscillations between 12 and 20 Hz (~900–1200ms; Figure 8a), tracked the retrieved  
531 location. Note, that in order to obtain the most robust measurement of spatially sensitive  
532 frequencies at retrieval, we only tested our IEM on trials from the second half of the experiment  
533 when memory performance and spatial selectivity were highest (Figure 6a). For consistency, we  
534 applied the same approach to study trials (Figure 6b). Applying the IEM to study trials revealed  
535 that spatially selective information was represented across a wider range of low frequencies  
536 (Figure 8b; 4–8 Hz, 0–500ms; 8–20 Hz, ~200–1750ms; 20–30 Hz, ~1500–1750ms) than during  
537 retrieval. However, we observed the most sustained spatial selectivity across the delay period in  
538 the alpha band (8–12 Hz). These results replicate past work showing that alpha-band activity  
539 tracks locations held in working memory (Sutterer et al., in press; Foster et al., 2016). Finally, an  
540 overlay plot of frequency bands carrying spatially specific information in both the encoding and  
541 retrieval tasks (Figure 8c), revealed considerable overlap in the 8–12 Hz band across conditions.  
542 Together these findings reveal that there is substantial, although not complete, overlap in the

543 range of frequencies carrying spatially specific information during memory encoding and  
544 retrieval.

545 [Insert Figure 8 here]

546 **Patterns of alpha-band activity generalize across encoding and retrieval.** While the  
547 same frequency band carried spatial information during both study and retrieval, this does not  
548 necessarily mean that the multivariate patterns of activity corresponding to each location are also  
549 similar during encoding and retrieval. To provide a comprehensive test of encoding-retrieval  
550 similarity, we trained the IEM using study trials and tested the model on retrieval trials. We  
551 observed robust spatial selectivity throughout the retrieval interval (520–1750ms;  $p < .05$ ; Figure  
552 9). This provides evidence that the multivariate pattern of alpha activity during retrieval is well-  
553 described as a re-instantiation of the pattern of alpha-band activity seen during encoding.

554 [Insert Figure 9 here]

555

## 556 **Discussion**

557 The present work represents a new approach for tracking and understanding the neural  
558 mechanisms underlying retrieval of precise feature memories. In two experiments, we employed  
559 a combination of a continuous report task, in which participants learned to associate individual  
560 objects with specific spatial locations, with the application of an inverted encoding model (IEM)  
561 to ongoing EEG activity. Using an IEM, we showed that rhythmic brain activity enables  
562 temporally resolved tracking of the retrieval of precise spatial locations from long-term memory.

563 A novel aspect of our work was the ability to search for frequencies that code for precise  
564 spatial memories. Recent theories about the role of neural oscillations in memory propose that  
565 both the frequencies supporting cognitive operations at encoding and retrieval and the specific

566 patterns of activity within those frequencies should overlap (Siegel et al., 2012; Watrous and  
567 Ekstrom, 2014; Watrous et al., 2015). In line with this prediction, we observed considerable  
568 overlap in the frequencies carrying spatial memory representations between encoding and  
569 retrieval. Specifically, we observed sustained spatial selectivity, primarily in the alpha band (8–  
570 12 Hz), during both study and long-term memory retrieval. We also found that the multivariate  
571 patterns of alpha-band activity reinstated during retrieval are similar to those patterns observed  
572 during the initial encoding of locations. These observations provide new evidence that encoding-  
573 retrieval oscillatory similarity extends to the representation of precise feature representations at  
574 the population level, supporting the idea that oscillatory brain activity plays a critical role in  
575 memory formation and reinstatement. However, it is worth noting that a broader range of  
576 frequencies tracked to-be-remembered locations at study than at retrieval, suggesting that not all  
577 spatially sensitive frequencies engaged during stimulus presentation are later reinstated.

578         The observation that alpha-band activity tracks retrieved spatial memories is similar to  
579 what has been observed during visual working memory maintenance (Sutterer et al., in press;  
580 Foster et al., 2016, 2017a), and is consistent with work that suggests a role for alpha in memory  
581 retrieval and memory guided attention (Stokes et al., 2012; Waldhauser et al., 2016; Fukuda and  
582 Woodman, 2017). However, this stands in contrast with other findings that suggest an important  
583 role of theta and beta activity in long-term memory. We observed relatively little spatial  
584 selectivity in the beta-band during memory retrieval, which is consistent with the notion that  
585 beta-band (15–25 Hz) activity may be more important for the encoding and retrieval of  
586 category-specific information (Morton et al., 2013; Morton and Polyn, 2017) rather than spatial  
587 information. While past studies have found that theta-band activity (4–7 Hz) plays a key role in  
588 episodic memory (Nyhus and Curran, 2010; Hsieh and Ranganath, 2014; Kerren et al., 2018) and

589 in the hippocampus during spatial navigation (Watrous et al., 2011; Bohbot et al., 2017), it is  
590 likely that our scalp EEG signal is insensitive to theta signals prominent in the  
591 hippocampus (Hsieh and Ranganath, 2014). Future work from modalities that more directly index  
592 hippocampal activity (i.e., intracranial recordings from the hippocampus) or use source  
593 reconstruction to isolate activity originating in the medial temporal lobe (Kerren et al., 2018)  
594 might provide insight into the role of theta activity in precise spatial memory reinstatement.

595         Another promising application of the approach employed here is the ability to compare  
596 the time course with which fine-grained and coarser memory representations emerge. For  
597 example, spatially selective alpha activity emerged considerably later than some prior  
598 observations of hemifield-selective activity. While hemifield selective activity has been observed  
599 within 200 ms of the onset of a retrieval cue (Waldhauser et al., 2016), our time by frequency  
600 analysis revealed no evidence of activity related to the specific retrieved location, in any  
601 frequency band, until at least 410 ms after the retrieval cue. One possible explanation for this  
602 latency difference is that hemisphere reactivation and retrieval of fine-grained spatial  
603 representations rely on different processes. For instance, Gratton and colleagues suggest that the  
604 hemisphere bias they observed may be more structural, resulting from the formation of a stronger  
605 trace in the hemisphere contralateral to the hemifield in which the stimulus was presented  
606 (Gratton et al., 1997). In the present study, the relatively slower onset of alpha CTFs implies a  
607 more effortful retrieval of precise spatial information. Another potential explanation is that  
608 context reinstatement during an object recognition task could occur more rapidly than object-  
609 cued retrieval of spatially selective information. Further work is needed to explore this difference  
610 in latency between hemifield effects and the reactivation of the fine-grained alpha topography  
611 that tracks specific locations.

612 We modeled LTM retrieval performance using a mixture modeling approach. This  
613 approach is commonplace in the field of visual working memory (Wilken and Ma, 2004; Zhang  
614 and Luck, 2008). More recently, this approach proven useful in the study of LTM (Brady et al.,  
615 2013; Harlow and Donaldson, 2013; Murray et al., 2015; Richter et al., 2016). A key advantage  
616 of the mixture modelling approach is that it provides distinct measures of mnemonic precision  
617 and the probability that memories are retrieved (Fan and Turk-Browne, 2013; Harlow and  
618 Yonelinas, 2016; Sutterer and Awh, 2016). Initial studies have found that these parameters are  
619 reflected by distinct neural signals (Murray et al., 2015; Richter et al., 2016), providing further  
620 evidence that separately modeling mnemonic precision and probability of retrieval is a  
621 meaningful distinction. Our results demonstrate that both the probability of retrieving long-term  
622 memories and the precision with which those memories are retrieved continue to improve with  
623 feedback over many repetitions. We propose that this more sensitive approach of assessing  
624 memory accuracy will shed new light on long-standing questions in the field.

### 625 **Does alpha-band activity reflect memory reinstatement?**

626 There is a considerable body of work demonstrating links between alpha-band activity  
627 and spatial attention (Worden et al., 2000; Foster et al., 2017b; Foster and Awh, 2019). Thus, it is  
628 possible that the spatial alpha-band representations we report here reflect sustained attention to  
629 studied and remembered locations. This raises the question of whether deployment of covert  
630 attention to a remembered location at retrieval qualifies as memory reinstatement. In our view, it  
631 does. Reinstatement is typically defined by consistent patterns of activity between encoding and  
632 retrieval (Danker and Anderson, 2010), and in the present study we observed that both the  
633 frequencies and patterns of activity engaged during initial encoding and are re-engaged during  
634 retrieval. We also note that it is well known that is possible to attend to features and categories.

635 Thus, most demonstrations of category or feature level reinstatement share a similar relationship  
636 with attention. In line with this idea, retro-cuing studies have demonstrated that categories  
637 (Lewis-peacock et al., 2011; Larocque et al., 2013; Rose et al., 2016) or features (Larocque et al.,  
638 2017) that must be attended to prepare for an upcoming test are uniquely decodable, while the  
639 features of items that are not necessary for the current probe cannot be decoded. Thus, past and  
640 present findings are consistent with the view that there is considerable overlap between attention  
641 and memory (Gazzaley and Nobre, 2012).

642 This tight coupling of memory and attention has inspired an active body of research  
643 exploring the extent that attention to a stimulus and attention guided by memory are supported  
644 by the same neural underpinnings (Summerfield et al., 2006). New fMRI evidence suggests that  
645 the networks supporting attention in these cases are not completely overlapping. For instance,  
646 hemispheric asymmetries observed in parietal cortex when observers attend a stimulus, are not  
647 observed when memory guides attention to a stimulus (Rosen et al., 2015), and memory guided  
648 attention engages a different constellation of cortical regions than stimulus guided  
649 attention (Rosen et al., 2017). The present work demonstrates that while differences exist in the  
650 brain networks that support stimulus and memory guided attention a similar constellation of  
651 oscillatory activity supports both processes.

## 652 **Conclusion**

653 Prominent models have argued that spatial-temporal context is the backbone of episodic  
654 memory (O'Keefe and Nadel, 1978; Ekstrom and Ranganath, 2018) serving as an index for the  
655 retrieval of specific past experiences. Thus, a method that allows temporally-resolved tracking of  
656 spatial retrieval from LTM may provide a powerful tool for understanding human memory. Here,  
657 we present such a method, and show that it tracks both the accuracy and latency of memory-

658 guided behavior. Moreover, we provide new evidence confirming a clear prediction of  
659 reinstatement models of LTM retrieval. The format of oscillatory activity during encoding into  
660 LTM is recapitulated during the subsequent retrieval of those memories.



661 **Funding**

662 This work was supported by National Institute of Mental Health Grant R01MH-08721406A1 to

663 E.A. and E.K.V.

664

665 **Acknowledgements**

666 The authors would like to thank Brendan Colson, Nicholas Diaz, Jared Evans, Ariana Gale,

667 Anubuv Gupta, Dylan Seitz, and William Ngiam for assistance with data collection, and Megan

668 deBettencourt for helpful comments on the manuscript.

669

670

671

672 **References**

- 673 Bohbot VD, Copara MS, Gotman J, Ekstrom AD (2017) Low-frequency theta oscillations in the  
674 human hippocampus during real-world and virtual navigation. *Nat Commun* 8:1–7.
- 675 Bosch SE, Jehee JFM, Fernandez G, Doeller CF (2014) Reinstatement of Associative Memories  
676 in Early Visual Cortex Is Signaled by the Hippocampus. *J Neurosci* 34:7493–7500.
- 677 Brady TF, Konkle T, Gill J, Oliva A, Alvarez GA (2013) Visual Long-Term Memory Has the  
678 Same Limit on Fidelity as Visual Working Memory. *Psychol Sci* 24:981–990.
- 679 Brainard DH (1997) The Psychophysics Toolbox. *Spat Vis* 10:433–436.
- 680 Brouwer GJ, Heeger DJ (2009) Decoding and reconstructing color from responses in human  
681 visual cortex. *J Neurosci* 29:13992–14003.
- 682 Cohen MX (2014) Analyzing neural time series data: theory and practice.
- 683 Danker JF, Anderson JR (2010) The ghosts of brain states past: remembering reactivates the  
684 brain regions engaged during encoding. *Psychol Bull* 136:87–102.
- 685 Delorme A, Makeig S (2004) EEGLAB: An open source toolbox for analysis of single-trial EEG  
686 dynamics including independent component analysis. *J Neurosci Methods* 134:9–21.
- 687 Ekstrom AD, Ranganath C (2018) Space, time, and episodic memory: The hippocampus is all  
688 over the cognitive map. *Hippocampus* 28:680–687.
- 689 Ester EFF, Sprague TCC, Serences JTT (2015) Parietal and Frontal Cortex Encode Stimulus-  
690 Specific Mnemonic Representations during Visual Working Memory. *Neuron* 87:897–905.
- 691 Fan JE, Turk-Browne NB (2013) Internal attention to features in visual short-term memory  
692 guides object learning. *Cognition* 129:292–308.
- 693 Favila SE, Samide R, Sweigart SC, Kuhl BA (2018) Parietal Representations of Stimulus  
694 Features Are Amplified during Memory Retrieval and Flexibly Aligned with Top-Down

- 695 Goals. *J Neurosci* 38:7809–7821.
- 696 Foster JJ, Awh E (2019) The role of alpha oscillations in spatial attention: limited evidence for a  
697 suppression account. *Curr Opin Psychol* 29:34–40.
- 698 Foster JJ, Bsaies EM, Jaffe RJ, Awh E (2017a) Alpha-Band Activity Reveals Spontaneous  
699 Representations of Spatial Position in Visual Working Memory. *Curr Biol* 27:3216–3223.
- 700 Foster JJ, Sutterer DW, Serences JT, Vogel EK, Awh E (2016) The topography of alpha-band  
701 activity tracks the content of spatial working memory. *J Neurophysiol* 115:168–177.
- 702 Foster JJ, Sutterer DW, Serences JT, Vogel EK, Awh E (2017b) Alpha-band oscillations enable  
703 spatially and temporally resolved tracking of covert spatial attention. *Psychol Sci* 28:929–  
704 941.
- 705 Fukuda K, Woodman GF (2017) Visual working memory buffers information retrieved from  
706 visual long-term memory. *Proc Natl Acad Sci* 114:5306–5311.
- 707 Gazzaley A, Nobre AC (2012) Top-down modulation: Bridging selective attention and working  
708 memory. *Trends Cogn Sci* 16:129–135.
- 709 Gratton G, Corballis PM, Jain S (1997) Hemispheric Organization of Visual Memories. *J Cogn*  
710 *Neurosci* 9:92–104.
- 711 Harlow IM, Donaldson DI (2013) Source accuracy data reveal the thresholded nature of human  
712 episodic memory. *Psychon Bull Rev* 20:318–325.
- 713 Harlow IM, Yonelinas AP (2016) Distinguishing between the success and precision of  
714 recollection. *Memory* 24:114–127.
- 715 Hindy NC, Ng FY, Turk-Browne NB (2016) Linking pattern completion in the hippocampus to  
716 predictive coding in visual cortex. *Nat Neurosci* 19:665–667.
- 717 Hsieh L-T, Ranganath C (2014) Frontal midline theta oscillations during working memory

- 718 maintenance and episodic encoding and retrieval. *Neuroimage* 85:721–729.
- 719 Jafarpour A, Fuentemilla L, Horner AJ, Penny W, Duzel E (2014) Replay of very early encoding  
720 representations during recollection. *J Neurosci* 34:242–248.
- 721 Johnson JD, Price MH, Leiker EK (2015) Episodic retrieval involves early and sustained effects  
722 of reactivating information from encoding. *Neuroimage* 106:300–310.
- 723 Kerren C, Linde-Domingo J, Hanslmayr S, Wimber M (2018) An Optimal Oscillatory Phase for  
724 Pattern Reactivation During Memory Retrieval. *SSRN Electron J*:1–10.
- 725 Larocque JJ, Lewis-Peacock J a, Drysdale AT, Oberauer K, Postle BR (2013) Decoding attended  
726 information in short-term memory: an EEG study. *J Cogn Neurosci* 25:127–142.
- 727 Larocque JJ, Riggall AC, Emrich SM, Postle BR (2017) Within-category decoding of  
728 information in different attentional states in short-term memory. *Cereb Cortex* 27:4881–  
729 4890.
- 730 Lewis-peacock JA, Drysdale AT, Oberauer K, Postle BR (2011) Neural Evidence for a  
731 Distinction between Short-term Memory and the Focus of Attention. *J Cogn Neurosci*  
732 24:61–79.
- 733 Lins OG, Picton TW, Berg P, Scherg M (1993) Ocular artifacts in recording EEGs and Event-  
734 Related potentials II: Source dipoles and source components. *Brain Topogr* 6:65–78.
- 735 Maris E, Oostenveld R (2007) Nonparametric statistical testing of EEG- and MEG-data. *J*  
736 *Neurosci Methods* 164:177–190.
- 737 Morton NW, Kahana MJ, Rosenberg E a, Baltuch GH, Litt B, Sharan AD, Sperling MR, Polyn  
738 SM (2013) Category-specific neural oscillations predict recall organization during memory  
739 search. *Cereb Cortex* 23:2407–2422.
- 740 Morton NW, Polyn SM (2017) Beta-band activity represents the recent past during episodic

- 741 encoding. *Neuroimage* 147:692–702.
- 742 Murray JG, Howie CA, Donaldson DI (2015) The neural mechanism underlying recollection is  
743 sensitive to the quality of episodic memory: Event related potentials reveal a some-or-none  
744 threshold. *Neuroimage* 120:298–308.
- 745 Nyhus E, Curran T (2010) Functional role of gamma and theta oscillations in episodic memory.  
746 *Neurosci Biobehav Rev* 34:1023–1035.
- 747 O’Keefe, Nadel L (1978) *The Hippocampus as a Cognitive Map*.
- 748 Pelli DG (1997) The VideoToolbox software for visual psychophysics: Transforming numbers  
749 into movies. *Spat Vis* 10:437–442.
- 750 Polyn SM, Natu VS, Cohen JD, Norman KA (2005) Category-specific cortical activity precedes  
751 retrieval during memory search. *Science* (80- ) 310:1963–1966.
- 752 Richter FR, Cooper RA, Bays PM, Simons JS (2016) Distinct neural mechanisms underlie the  
753 success, precision, and vividness of episodic memory. *Elife* 5:1–18.
- 754 Ritchey M, Wing EA, LaBar KS, Cabeza R (2013) Neural Similarity Between Encoding and  
755 Retrieval is Related to Memory Via Hippocampal Interactions. *Cereb Cortex* 23:2818–  
756 2828.
- 757 Rose NS, Larocque JJ, Riggall AC, Gosseries O, Starrett MJ, Meyering EE, Postle BR (2016)  
758 Reactivation of latent working memories with transcranial magnetic stimulation. *Science*  
759 (80- ) 354:1136–1139.
- 760 Rosen ML, Stern CE, Devaney KJ, Somers DC (2017) Cortical and Subcortical Contributions to  
761 Long-Term Memory-Guided Visuospatial Attention. *Cereb Cortex* 28:2935–2947.
- 762 Rosen ML, Stern CE, Michalka SW, Devaney KJ, Somers DC (2015) Influences of Long-Term  
763 Memory-Guided Attention and Stimulus-Guided Attention on Visuospatial Representations

- 764 within Human Intraparietal Sulcus. *J Neurosci* 35:11358–11363.
- 765 Saproo S, Serences JT (2014) Attention Improves Transfer of Motion Information between V1  
766 and MT. *J Neurosci* 34:3586–3596.
- 767 Siegel M, Donner TH, Engel AK (2012) Spectral fingerprints of large-scale neuronal  
768 interactions. *Nat Rev Neurosci* 13:121–134.
- 769 Sprague TC, Ester EF, Serences JT (2014) Reconstructions of information in visual spatial  
770 working memory degrade with memory load. *Curr Biol* 24:2174–2180.
- 771 Sprague TC, Ester EF, Serences JT (2016) Restoring latent visual working memory  
772 representations in human cortex. *Neuron* 91:694–707.
- 773 Sprague TC, Saproo S, Serences JT (2015) Visual attention mitigates information loss in small-  
774 and large-scale neural codes. *Trends Cogn Sci* 19:215–226.
- 775 Sprague TC, Serences JT (2013) Attention modulates spatial priority maps in the human  
776 occipital, parietal and frontal cortices. *Nat Neurosci* 16:1879–1887.
- 777 Stokes MG, Atherton K, Patai EZ, Nobre AC (2012) Long-term memory prepares neural activity  
778 for perception. *Proc Natl Acad Sci* 2011:188–197.
- 779 Suchow JW, Brady TF, Fougny D, Alvarez GA (2013) Modeling visual working memory with  
780 the MemToolbox. *J Vis* 13:1–8.
- 781 Summerfield JJ, Lepsien J, Gitelman DR, Mesulam MM, Nobre AC (2006) Orienting attention  
782 based on long-term memory experience. *Neuron* 49:905–916.
- 783 Sutterer DW, Awh E (2016) Retrieval practice enhances the accessibility but not the quality of  
784 memory. *Psychon Bull Rev* 23:831–841.
- 785 Sutterer DW, Foster JJ, Adam KCS, Vogel EK (n.d.) Item-specific delay activity demonstrates  
786 concurrent storage of multiple active neural representations in working memory. *PLoS Biol.*

- 787 Wagner AD, Shannon BJ, Kahn I, Buckner RL (2005) Parietal lobe contributions to episodic  
788 memory retrieval. *Trends Cogn Sci* 9:445–453.
- 789 Waldhauser GT, Braun V, Hanslmayr S (2016) Episodic Memory Retrieval Functionally Relies  
790 on Very Rapid Reactivation of Sensory Information. *J Neurosci* 36:251–260.
- 791 Watrous AJ, Ekstrom AD (2014) The Spectro-Contextual Encoding and Retrieval Theory of  
792 Episodic Memory. *Front Hum Neurosci* 8:1–15.
- 793 Watrous AJ, Fell J, Ekstrom AD, Axmacher N (2015) More than spikes: Common oscillatory  
794 mechanisms for content specific neural representations during perception and memory. *Curr*  
795 *Opin Neurobiol* 31:33–39.
- 796 Watrous AJ, Fried I, Ekstrom AD (2011) Behavioral correlates of human hippocampal delta and  
797 theta oscillations during navigation. *J Neurophysiol* 105:1747–1755.
- 798 Wheeler ME, Petersen SE, Buckner RL (2000) Memory's echo: Vivid remembering reactivates  
799 sensory-specific cortex. *J Neurosci* 20:11125–11129.
- 800 Wilken P, Ma WJ (2004) A detection theory account of change detection. *J Vis* 4:1120–1135.
- 801 Wimber M, Maaß A, Staudigl T, Richardson-Klavehn A, Hanslmayr S (2012) Rapid memory  
802 reactivation revealed by oscillatory entrainment. *Curr Biol* 22:1482–1486.
- 803 Worden MS, Foxe JJ, Wang N, Simpson G V (2000) Anticipatory biasing of visuospatial  
804 attention indexed by retinotopically specific alpha-band electroencephalography increases  
805 over occipital cortex. *J Neurosci* 20:1–6.
- 806 Xiao X, Dong Q, Gao J, Men W, Poldrack RA, Xue G (2017) Transformed Neural Pattern  
807 Reinstatement during Episodic Memory Retrieval. *J Neurosci* 37:2986–2998.
- 808 Zhang W, Luck SJ (2008) Discrete fixed-resolution representations in visual working memory.  
809 *Nature* 453:233–235.

810

811



812 **Figure 1. Task figure and memory performance for Experiments 1 and 2. A.** Schematic of  
813 Experiment 1, with example study (Experiment 1, Day 1) and retrieval (Experiment 1, Day 2)  
814 trials. Each trial was initiated with a space press. **B.** Average absolute error of retrieval responses  
815 demonstrating improvements over retrieval repetitions. **C.** Schematic of interleaved study and  
816 retrieval repetitions in Experiment 2 with example study and retrieval trials. Each trial was  
817 initiated with a space press. **D.** Average absolute error of study and retrieval responses  
818 demonstrating memory accuracy over study and retrieval repetitions. Error bars represent  $\pm 1$   
819 s.e.m.  
820

821 **Figure 2. Alpha band (8–12 Hz) channel tuning functions (CTF) from Experiment 1.**

822 **A.** Alpha CTF across time. An IEM was used to reconstruct spatially selective CTFs from the  
823 topographic distribution of alpha-band power. CTF selectivity was reliable from 588 to 1250ms  
824 (quantified as CTF slope;  $p < .05$ , indicated by the black marker). **B.** Alpha CTF derived with a  
825 set of 8 delta functions and averaged across significant time points (588–1250 ms). Delta  
826 function CTFs are graded confirming that the signal carried by the topography of alpha band  
827 power is intrinsically graded. Thus, the use of a graded basis set is appropriate. Shaded area  
828 represents  $\pm 1$  bootstrapped s.e.m. **C.** Alpha CTF derived with a graded basis set and averaged  
829 across significant time points (588–1250 ms). Shaded area represents  $\pm 1$  s.e.m. **D.** Channel  
830 responses for each of the eight stimulus location bins averaged across significant time points  
831 (588–1250ms). The channel response peaks at the channels preferred location, indicating that  
832 alpha activity is selective for the specific remembered location.

833

834 **Figure 3. Identifying frequencies that track retrieved locations for Experiment 1.**

835 **A.** An IEM was used to reconstruct spatially selective CTFs from the topographic distribution of  
836 total power across a range of frequencies (4–50Hz). Alpha power tracked retrieval of spatial  
837 information. **B.** Training and testing across shapes. Alpha power continued to track the retrieval  
838 of spatial information when the IEM was trained and tested on separate shape cues, indicating  
839 that CTFs reflect remembered locations not the retrieval cue. Points at which CTF slope values  
840 were not reliably above zero as determined by a cluster corrected permutation test ( $p < .05$ ) were  
841 set to dark blue.

842

843 **Figure 4. Assessing the relationship between alpha selectivity and memory performance for**  
844 **Experiment 1. A.** Average response error improved from the first to the second half of the  
845 experiment ( $p < .001$ ). Error bars represent  $\pm 1$  s.e.m. **B.** Time resolved CTF slopes for trials from  
846 the first and second half of the experiment. CTF slope reflects learning across the session and  
847 reveals significantly higher spatial selectivity for the second half of the experiment relative to the  
848 first half ( $p = .003$ ). Reliable differences were assessed by averaging across time points where we  
849 observed reliable CTFs for all trials (grey box) and comparing CTF slope between the first and  
850 second half of the experiment. Shaded error bars represent  $\pm 1$  s.e.m.  
851

852 **Figure 5. Assessing the relationship between alpha selectivity and response times for**  
853 **Experiment 1. A.** Aggregate distribution of all participants' fast and slow response times.  
854 Response times > 7s are represented in the last bin of the histogram. **B.** Time resolved CTF slope  
855 for trials with the fastest and slowest response times. CTF slope reflects response latency and  
856 reveals that spatial selectivity was higher for trials when participants responded quickly  
857 ( $p < .001$ ). Reliable differences were assessed by averaging CTF slope across time points where  
858 we observed reliable CTFs for all trials (grey box) and comparing CTF slopes for slow and fast  
859 trials. Shaded error bars represent  $\pm 1$  s.e.m. **C.** Alpha selectivity is modestly correlated with  
860 response times across subjects although the relationship is not significant ( $\rho(26) = -.36$   $p = .07$ ).  
861

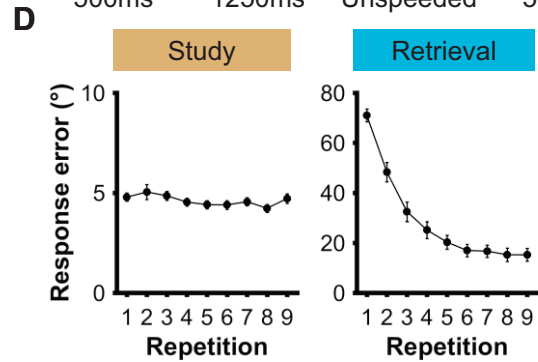
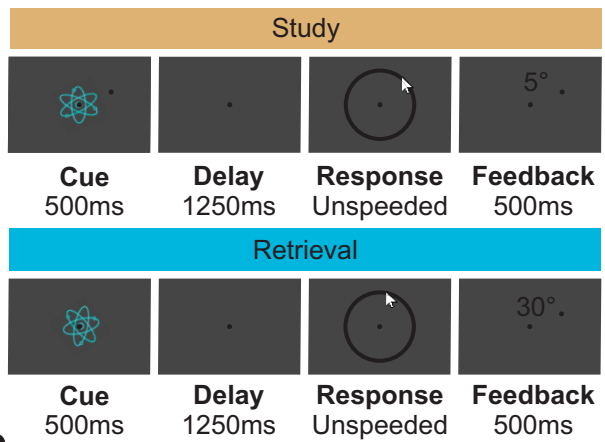
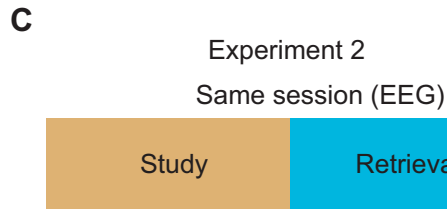
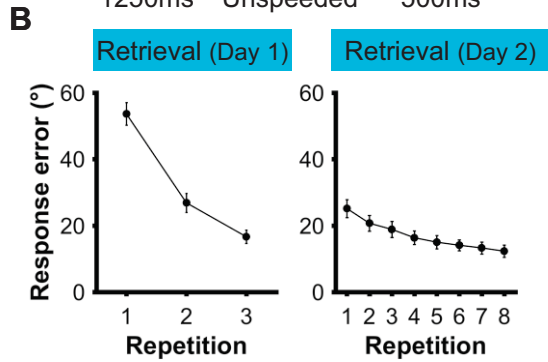
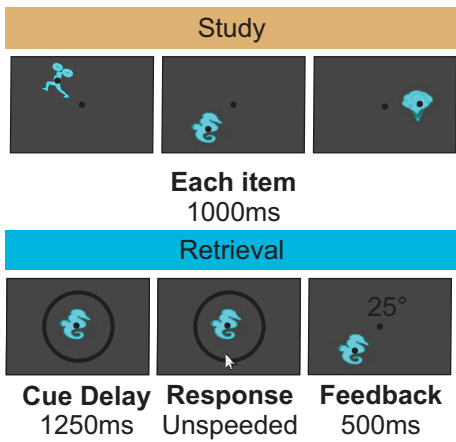
862 **Figure 6. Assessing the relationship between alpha selectivity and memory performance for**  
863 **Experiment 2. A.** Average response error improved from the first to the second half of the  
864 experiment ( $p < .001$ ). Error bars represent  $\pm 1$  s.e.m. **B.** Time resolved CTF slopes for trials  
865 from the first and second half of the experiment. CTF slope reflects learning across the session  
866 and reveals significantly higher spatial selectivity for the second half of the experiment relative  
867 to the first half ( $p < .001$ ). Reliable differences were assessed by averaging across time points  
868 where we observed reliable CTFs for all trials (grey box) and comparing CTF slope between the  
869 first and second half of the experiment. Shaded error bars represent  $\pm 1$  s.e.m.  
870

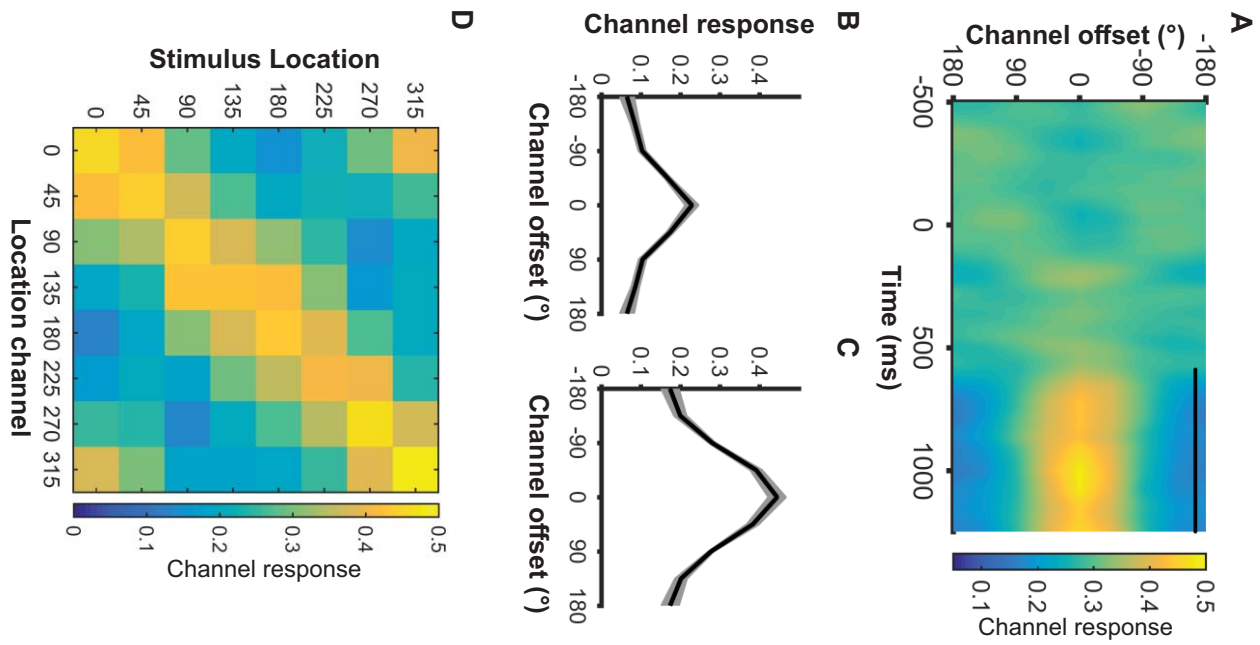
871 **Figure 7. Assessing the relationship between alpha selectivity and response times for**  
872 **Experiment 2. A.** Aggregate distribution of all participants' fast and slow response times.  
873 Response times > 7s are represented in the last bin of the histogram. **B.** Time resolved CTF slope  
874 for trials with the fastest and slowest response times. CTF slope reflects response latency and  
875 reveals that spatial selectivity was higher for trials when participants responded quickly ( $p=.018$ ).  
876 Reliable differences were assessed by averaging CTF slope across time points where we  
877 observed reliable CTFs (grey box) for all trials and comparing fast and slow trials. Shaded error  
878 bars represent  $\pm 1$  s.e.m. **C.** Alpha selectivity is modestly correlated with response times across  
879 subjects ( $\rho(23) = -.49$   $p = .02$ ).  
880

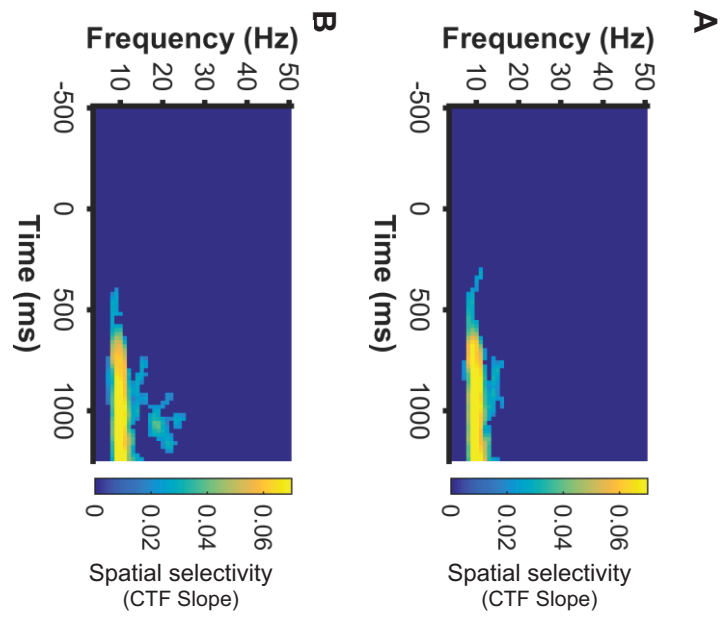
881 **Figure 8. Identifying frequencies that track encoded and retrieved locations for**  
882 **Experiment 2.** An IEM was used to reconstruct spatially selective CTFs from the topographic  
883 distribution of total power across a range of frequencies (4–50Hz) at retrieval and study. To  
884 ensure robust retrieval memory performance, only trials from the second half of the session were  
885 used in the test set for this analysis. **A.** Primarily alpha power tracked spatial information during  
886 retrieval trials. **B.** Initially, a broad range of frequencies tracked the encoded location (4–35Hz)  
887 while primarily alpha power tracked the remembered location through the entire delay. **C.**  
888 Overlay plot of significant activity during retrieval and study. Teal points reflect reliable spatial  
889 selectivity during study, orange points reflect reliable selectivity at retrieval, and magenta points  
890 reflect overlap selectivity at study and retrieval. Points at which CTF slope values were not  
891 reliably above zero as determined by a cluster corrected permutation test ( $p < .05$ ) were set to  
892 dark blue.  
893

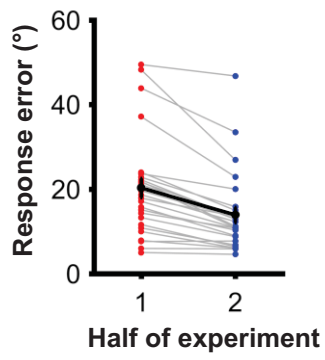
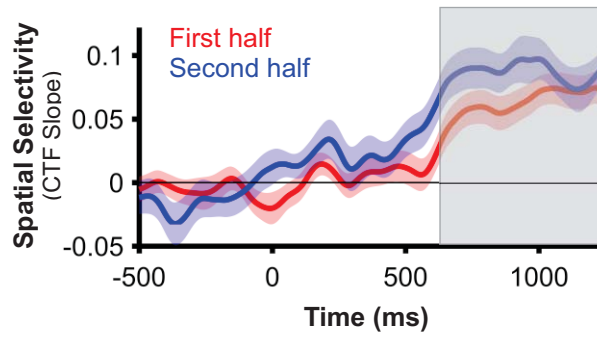


894 **Figure 9. Testing whether the multivariate patterns of alpha power at study are reinstated**  
895 **at retrieval.** Alpha power tracks the retrieval of spatial information when the IEM was trained  
896 on study data and tested on retrieval data, indicating that the pattern of alpha band activity  
897 observed during study is reactivated at retrieval. Shaded error bars represent  $\pm 1$  s.e.m. Markers  
898 on the top of the plot mark the periods of reliable spatial selectivity ( $p < .05$ ).

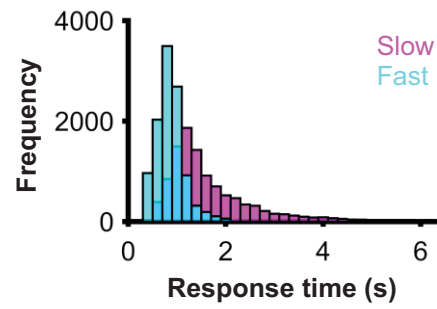




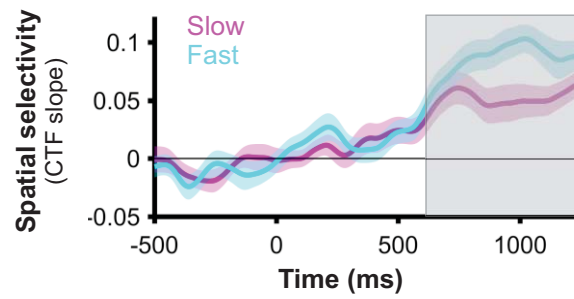


**A****B**

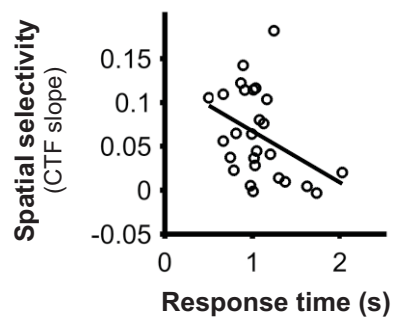
**A** Aggregate RT Distributions

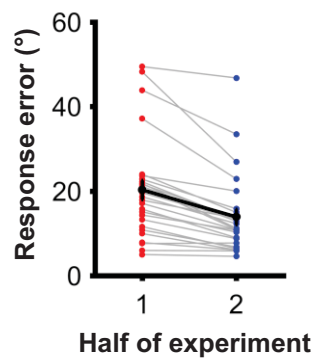
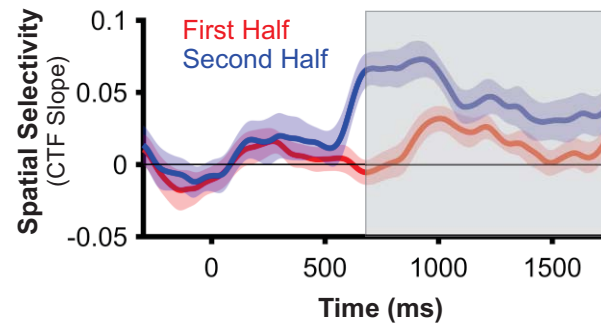


**B**

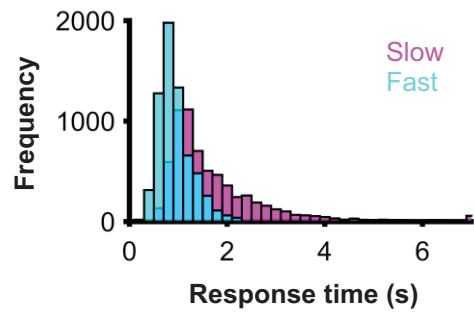


**C**

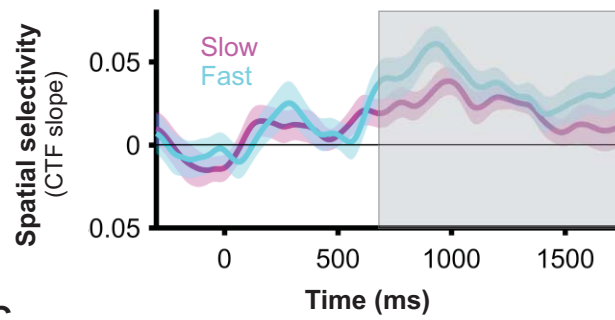


**A****B**

**A** Aggregate RT Distributions



**B**



**C**

